PHOTOPROTONS FROM FLUORINE

By W. B. Lasich,* E. G. Muirhead,† and G. G. Shute†

[*Manuscript received August* 31, 1955]

Summary

The energy and angular distributions of protons produced in the ^{19}F (γ, p) reaction have been obtained for the photon energy range 10–16·5 MeV. An integrated cross section of 18 MeV-mbarn was obtained for this region. The angular distribution was found to be of the form $(a+b \sin^2 \theta)$ with the ratio b/a strongly energy dependent. The higher energy protons show evidence of an independent particle-type interaction which is in plausible agreement with the shell model structure of fluorine.

The range-energy relation for the target gas, CF_4, is presented in Appendix I.

I. Introduction

Recent experiments on photonuclear reactions have been directed towards elucidating the mechanisms of photon absorption by nuclei undergoing photodisintegration. Photoneutron production in light nuclei has been studied by Katz *et al.* (1954) and Penfold and Spicer (1955) who showed that, for the (γ, n) reactions studied, photons excite the nucleus predominantly by level absorption with the formation of a compound nucleus state. The absorption is probably electric quadrupole or magnetic dipole in character at excitation energies immediately above the binding energy of the nucleon being ejected, changing to electric dipole as the region of the " giant resonance " is approached. The relative importance of the compound nucleus formation and the alternative direct or independent-particle interaction (Courant 1951, Wilkinson 1955) has yet to be determined, especially for light nuclei. In the case of carbon the protons ejected at the giant resonance at 22 MeV were found to have an angular distribution as predicted by the independent-particle model (Mann, Stephens, and Wilkinson 1955).

Experiments on the photodisintegration of light nuclei are particularly suitable for the study of photon absorption, since the level density in the excited nucleus is still small enough to permit the resolution of products coming from discrete energy levels. Much of the experimental work relevant to this problem has been summarized by Titterton (1955).

The present experiment was undertaken to study the production of photoprotons from a light nucleus. Fluorine was chosen because of its low proton binding energy and also because it is free of complications arising from the presence of more than one isotope. A gas target was considered preferable for the measurement of angular distributions, and a suitable gas, tetrafluoromethane

* Australian Atomic Energy Commission, University of Melbourne.
† Physics Department, University of Melbourne.

(CF_4), was found to be available commercially with a high degree of purity. The energy and angular distributions of protons from fluorine were obtained for the photon region 10–16·5 MeV using the X-ray beam from the Melbourne synchrotron and a reaction chamber containing nuclear emulsions.

II. Experimental

The X-rays were produced from a conventional betatron target, a 0·005 in. platinum flag. The beam was reduced to an angular width of 0·022 radian by a lead collimator, and then passed through a 0·001 in. aluminium window into the reaction chamber. Here the mean beam diameter was 1·7 cm as determined by radiographs taken on the emergent side of the chamber. The reaction chamber, based on the design of Fuller (1950), was used previously by Spicer (1953) for the $^{14}N(\gamma, p)$ reaction. The gas target was maintained at a pressure of half an atmosphere. Two 100 μ C2 emulsions were placed relative to the beam as shown in Figure 1. The data were taken from two runs, each

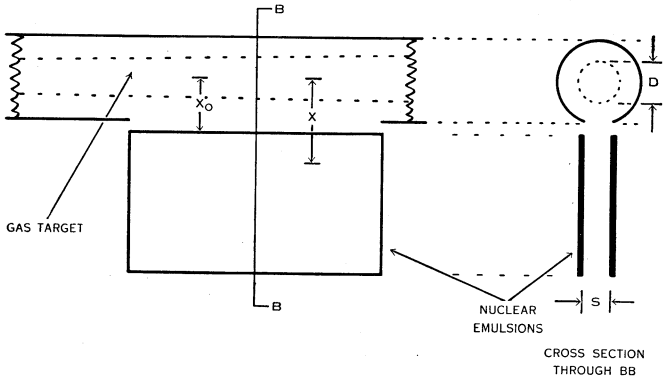

Fig. 1.—Positioning of nuclear emulsions relative to X-ray beam. Mean beam diameter, D = 1·7 cm ; emulsion spacing, S = 1·3 cm ; beam centre to emulsion, X_0 = 2·3 cm ; beam centre to average swathe, X = 3·7 cm.

target irradiation being approximately 1100 r. The chamber was surrounded by 20 cm of paraffin and a similar thickness was placed between the doughnut and the collimator to reduce the neutron background. However, the X-ray beam was allowed to pass through a 1·5 cm hole in the paraffin so as to preserve more closely the " thin " target spectral distribution. The exposure was obtained from the readings of a 25 r Victoreen thimble contained in an 8 cm " Perspex " cube, the latter being placed in the beam opposite the exit end of the reaction chamber. The photon flux through the chamber was deduced from this " Lucite-roentgen " reading using the tables of Katz and Cameron (1951).

The synchrotron energy scale was calibrated from the ratio of induced activities in copper and silver using the activation curves of Diven and Almy (1950), and allowed the peak energy of the X-ray distribution to be determined as 16·5 ± 0·5 MeV. Track measurements on the emulsions were made on Cooke,

Troughton, and Simms model 4000 microscopes, a 45× objective with 8× eyepiece giving a convenient size field of some 200 μ diameter. Tracks were accepted from swathes of 160 μ width so as to avoid possible bias in the angular distributions due to loss of tracks commencing near the periphery of the field of view. The usual angle, range, and dip measurements were recorded for each track. The criterion for acceptance of a track was that it should appear to cross the emulsion surface and have a direction and dip compatible with an origin in the irradiated part of the gas target. Using selected areas on the emulsions, tracks were accepted for angles θ, in the range 30–150° with a dip angle, δ°, satisfying the condition,

$$\delta \leqslant 24 \sin \theta \, (3{\cdot}5/X), \quad \ldots\ldots\ldots\ldots\ldots \quad (1)$$

where X is the beam-swathe distance in cm as defined in Figure 1, and θ is the angle between the incident photon and the proton.

The range of each proton accepted as coming from the target was determined from the known geometrical set-up of the emulsions relative to the beam. To obtain each proton energy, the range-energy relations used were (i) the tables of Wilkins (1951) for C2 emulsions, and (ii) the table for CF_4 presented in Appendix I (Table 4). In practice, it was found convenient to convert the residual range in the emulsion to the CF_4 gas range of a proton with equivalent energy, which, when added to range in the gas target, permitted the tracks for the energy distribution to be grouped according to the total equivalent gas range.

The main uncertainty in the determination of proton energies was due to the finite thickness of the gas target used. In accumulating tracks for the energy and angular distributions, different criteria were required in order to preserve good energy resolution in the one case and adequate angular coverage in the other. Since the effective thickness of the target depended on cosec θ, the data for the energy spectrum were restricted to the range of θ from 45 to 135°. The uncertainty in proton energy arising from the target thickness varied from 7 per cent. for 2 MeV protons to 1·7 per cent. for 6 MeV tracks. In addition, proton range straggling amounted to 2–3 per cent. The resulting overall uncertainty in energy ranged from ∼0·15 MeV for 2 MeV protons, to ∼0·12 MeV for 6 MeV protons. Hence it was not possible to demonstrate the existence of distinct proton groups with energies closer than approximately 0·3 MeV.

For the angular distribution, on the other hand, the lower limit for the acceptance of tracks was set in principle by the minimal residual range in the emulsion which would be easily identified by an observer. This was set at a range of 12 μ (0·9 MeV), which, together with the angular limits used (30–150°), resulted in a lower limit for the proton energy of 2·5 MeV. The angular distribution, plotted for 15° intervals of θ, was obtained from the relation between the relative differential cross section dσ, and the number of tracks $N(\theta)$ per 15° interval (Fuller 1950):

$$N(\theta) = \text{const. } d\sigma \, \overline{\sin \theta}, \quad \ldots\ldots\ldots\ldots\ldots \quad (2)$$

with $\overline{\sin \theta}$ the corresponding mean value of sin θ for each 15° interval.

Background tracks arose from two possible sources: (i) those generated in the beam region due to reactions other than the $^{19}F(\gamma, p)$ reaction, and (ii) those produced in the emulsions as neutron-proton recoils.

The thresholds for the majority of type (i) reactions are given in Table 1. The thresholds for (n, p) reactions in carbon and fluorine are such that the number of protons produced which would reach the emulsions was negligible. In fluorine, for example, using an estimate of the flux and energy distribution of fast neutrons from an X-ray target (Wäffler 1954), it was shown that the number of protons produced in the (n, p) reaction with energy sufficient to reach the emulsions was of the order 10^{-5} times the expected number of photoprotons.

TABLE 1

THRESHOLDS FOR POSSIBLE COMPETING REACTIONS

Reaction	Threshold (MeV)	Reference
$^{19}F(\gamma, p)$	7·97	Drummond (1955)
$^{19}F(\gamma,d)$	13·80	,,
$^{19}F(\gamma,t)$	11·69	,,
$^{19}F(\gamma,\alpha)$	4·01	,,
$^{19}F(\gamma,np)$	16·02	,,
$^{12}C(\gamma,p)$	15·94	,,
$^{12}C(\gamma,d)$	25·17	,,
$^{12}C(\gamma,\alpha)$	7·36	,,
$^{19}F(n,p)$	3·72	Ajzenberg and Lauritsen (1955)
$^{12}C(n,p)$	12·6	,, ,,

Of the other reactions, photoprotons produced in the carbon failed to reach the emulsions, for the peak irradiation energy of 16·5 MeV chosen for this experiment. Likewise, the stopping power of the gas was sufficient to prevent the recording of deuterons and tritons ejected from fluorine. Preliminary runs showed that a significant number of tracks recorded came from the brass walls of the reaction chamber; accordingly, the latter was lined completely with graphite walls $\frac{1}{8}$ in. thick.

An estimate of the background tracks of type (ii) crossing the surface was made during the course of scanning. The number of tracks in the range $\theta = 210$–$330°$ was recorded. It was not possible to identify the direction of individual tracks but the majority was shown by the following method to have started in the emulsion. The average volume density of tracks was determined from sample counts made at various depths in the emulsion. Using this, an estimate of the number of tracks leaving the emulsion was made and this agreed with the number observed at the upper surface. The contribution of these protons to the total number of tracks observed in the acceptance sector ($\theta = 30$–$150°$) was calculated by assuming the distribution of the background to be symmetrical about a direction parallel to the beam axis. The distribution so obtained was consistent with an independent estimate obtained by scanning

a sample area ($=0\cdot36$ cm^2) and recording all tracks appearing to cross the emulsion surface with $\theta=30$–$150°$. A chart was prepared showing the distribution of tracks with large angles of dip ($\delta=30$–$60°$) and all possible values of θ. From the space distribution in δ the number of tracks occurring in the allowed dip region given by equation (**1**) was deduced. This estimate agreed within 10 per cent. with the former estimate, i.e. within the statistical error associated with a sample of 156 tracks.

In order to subtract the background, the same set of operations was performed on the background sample as for the main group of tracks. A fictitious energy was assigned to each background track, i.e. the energy which would be possessed by a photoproton of similar range and dip and with angle equal to $360°-\theta$. The same dip criterion (equation (**1**)) was also applied so as to have the same solid angle weighting factor for both sets of data. The backgrounds determined in this way were subtracted from each of the energy and angular distributions, as given in Figures 2 and 3.

III. Results

(*a*) *Energy Distribution*

Figure 2 (*a*) shows the number of photoprotons with energy greater than 2 MeV obtained from an emulsion area of $4\cdot8$ cm^2 *after* the subtraction of background. The latter is presented for reference in Figure 2 (*b*). The limit of resolution for discrete proton groups is about $0\cdot3$ MeV. For reference, the positions of every proton energy group expected from the known level structure in ^{19}F and ^{18}O are indicated by arrows in Figure 2 (*a*). The poor resolution and statistics prevent any correlation between these positions and the observed data to be established.

(*b*) *Angular Distribution*

The angular distributions for the two proton energy groups, $4\cdot4$–$8\cdot5$ MeV and $2\cdot9$–$4\cdot4$ MeV, are presented in Figures 3 (*a*) and 3 (*b*) respectively. The division at $4\cdot4$ MeV was made to obtain a sufficiently large sample of higher energy protons for an angular distribution. The lower limit of $2\cdot9$ MeV was taken in order to reduce the effect of background. In this way the percentage backgrounds for the higher and lower energy groups were 10 and $13\frac{1}{2}$ respectively. The simplest theoretical form of the angular distribution for the data is of the form $a+b\sin^2\theta$, since there is no apparent forward asymmetry in the data. A least squares fit for each group resulted in the smooth curves shown in Figure 3. The higher energy group can best be fitted, within the statistical uncertainties, by a $\sin^2\theta$ distribution, while the lower energy group tends more towards isotropy.

(*c*) *Integrated Cross Section*

It is not possible to obtain a precise value for the integrated cross section for the ^{19}F$(\gamma, p)^{18}$O reaction from the proton energy distribution without more detailed knowledge of the levels in ^{18}O. At present there is evidence for levels at $1\cdot98$ MeV and possibly at $2\cdot42$ MeV (Ajzenberg and Lauritsen 1955).

However, a lower limit can be derived from Figure 2 by assuming that all proton groups were due to transitions to the ^{18}O ground state only. The energy of each corresponding photon can then be determined from the relation

$$E=\frac{19}{18}E_p+7\cdot95, \quad \ldots\ldots\ldots\ldots\ldots \quad (3)$$

and the integrated cross section is obtained from the relation

$$N(E_0)=k\,\overline{P(E,E_0)}\int_{10}^{16\cdot5}\sigma(E)\mathrm{d}E, \quad \ldots\ldots\ldots\ldots \quad (4)$$

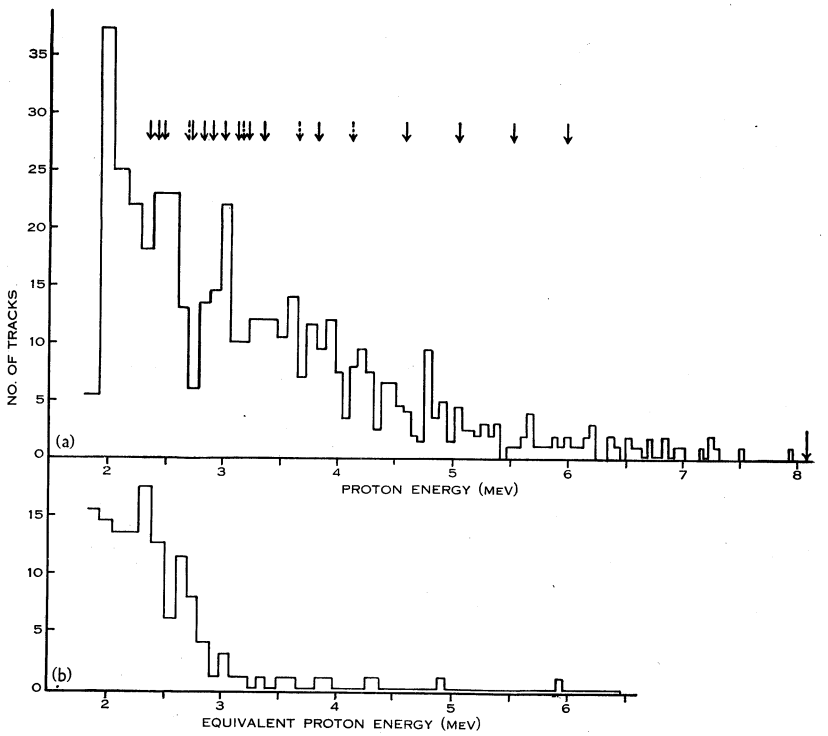

Fig. 2 (*a*).—Energy distribution of photoprotons from ^{19}F. The expected positions of proton groups between known energy levels in ^{19}F and ^{18}O are indicated by arrows above the histogram as follows:

↓ $^{19}F^*$ to ^{18}O (ground state),
⇣ $^{19}F^*$ to $^{18}O^*$ (1·98 MeV state).

(The energy levels in ^{19}F were observed in $^{18}O(p,n)^{18}F$ (Ajzenberg and Lauritsen 1955).) The limit of resolution is 0·3 MeV.

Fig. 2 (*b*).—Corresponding background tracks.

where $N(E_0)$ is the number of photoprotons in Figure 3 and $\overline{P(E,E_0)}$ is the average value of the photon flux per $\frac{1}{2}$ MeV interval between 10 and 16·5 MeV as taken from the tables of Katz and Cameron (1951). The value of k ($=1\cdot86\times10^{21}$) for the present experiment was obtained from the geometry of the chamber, the operating conditions, and the assumed angular distributions

for the groups in Figure 3. The result so obtained was 6 MeV-mbarn. This value is unrealistic owing to the probable importance of the 1·98 MeV level with $J=2$ in ^{18}O. In a similar way, an upper limit to the integrated cross section, assuming that where energetically possible all protons involved transitions to this state, leads to the value of 19 MeV-mbarn. Making the crude assumption that the relative importance of the ground and first excited states in ^{18}O is the ratio of their statistical weights, i.e. 1 : 5, gives a provisional estimate of the integrated cross section as 18 MeV-mbarn for the photon energy region 10–16·5 MeV.

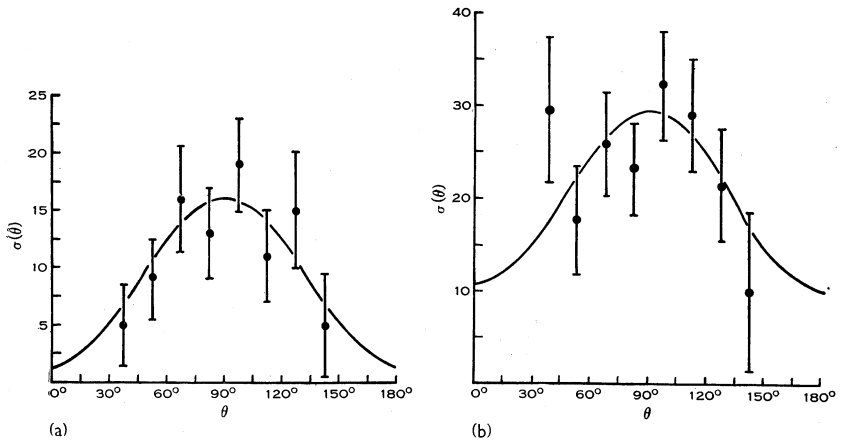

Fig. 3.—Angular distribution of photoprotons from ^{19}F. θ=angle between incident photon and the proton, $\sigma(\theta)$=differential cross section (arbitrary units). Vertical lines represent standard deviations of the points.

(*a*) Energy range 4·4–8·5 MeV. No. of tracks=75, percentage background=10, least squares fit to data is shown by curve $(1\pm5)+(15\mp7)\sin^2\theta$.

(*b*) Energy range 2·9–4·4 MeV. No. of tracks=180, percentage background=13½, least squares fit to data is shown by curve $(10\pm8)+(19\mp11)\sin^2\theta$.

For the reasons mentioned above, it is not possible to estimate the variation of cross section within the region studied. However, making the same assumption as for the integrated cross section, it can be shown that the cross section decreases monotonically with energy by a factor of two within the range under consideration.

IV. Interpretation

The angular distributions of photoprotons presented in Figure 3 can be represented by the expression $(a+b\sin^2\theta)$ with a and b positive or zero. It is of interest to compare the experimental distributions with those predicted for the process involving the formation of compound nucleus states in ^{19}F with assumed values of spin and parity. These are presented in Tables 2 and 3 for the ground and first excited states of ^{18}O. For the lower energy group (Fig. 3 (*b*)), the experimental angular distribution is more nearly consistent with E1 or M1 absorption with transitions to the ^{18}O ground state (Table 2), depending on whether the levels available in ^{19}F with spin 3/2 have negative or positive parity in the energy region considered. It does not seem plausible to fit these data

TABLE 2

THEORETICAL ANGULAR DISTRIBUTION FOR $^{19}F(\gamma,p)^{18}O$ REACTION FOR TRANSITIONS TO THE GROUND STATE ONLY

$I=\frac{1}{2}+$ throughout†

Type of Photon Absorption	L	J	l'	s'	$\sigma(\theta)$
E1	1	$\frac{1}{2}-$	1	$\frac{1}{2}+$	isotropic
E1	1	3/2—	1	$\frac{1}{2}+$	$2+3s^2$
M1	1	$\frac{1}{2}+$	0	$\frac{1}{2}+$	isotropic
M1	1	3/2+	2	$\frac{1}{2}+$	$2+3s^2$
E2	2	3/2+	2	$\frac{1}{2}+$	$1+c^2$
E2	2	5/2+	2	$\frac{1}{2}+$	$1+6c^2-5c^4$

† Here I=spin of initial state of ^{19}F $(=\frac{1}{2}+)$,
J=spin of the excited state, $^{19}F^*$,
L=angular momentum of incoming photon,
l'=angular momentum of emitted proton,
s'=final channel spin,
$c=\cos\theta$,
$s=\sin\theta$.

TABLE 3

THEORETICAL ANGULAR DISTRIBUTIONS FOR $^{19}F(\gamma,p)^{18}O$ REACTION FOR TRANSITIONS TO THE FIRST EXCITED STATE OF ^{18}O AT 1·98 MeV

$I=\frac{1}{2}+$ throughout*

Type of Absorption	L	J	l'	s'	$\sigma(\theta)$
E1	1	$\frac{1}{2}-$	1	3/2+	Isotropic
	1	$\frac{1}{2}-$	3	5/2+	Isotropic
	1	3/2−	1	3/2+	$4+3c^2$
	1	3/2−	1	5/2+	$21-3c^2$
	1	3/2−	3	5/2+	$19+3c^2$
M1	1	$\frac{1}{2}+$	2	3/2+	Isotropic
	1	$\frac{1}{2}+$	2	5/2+	Isotropic
	1	3/2+	0	3/2+	Isotropic
	1	3/2+	2	5/2+	$23+15c^2$
	1	3/2+	4	5/2+	$33-15c^2$
E2	2	3/2+	0	3/2+	Isotropic
	2	3/2+	2	3/2+	Isotropic (accidentally)
	2	3/2+	2	5/2+	$33-15c^2$
	2	3/2+	4	5/2+	$23+15c^2$
	2	5/2+	2	3/2+	$56-105c^2+140c^4$
	2	5/2+	4	3/2+	$119+420c^2-315c^4$
	2	5/2+	0	5/2+	Isotropic
	2	5/2+	2	5/2+	$189+210c^2-315c^4$
	2	5/2+	4	5/2+	$203-210c^2+315c^4$

* See footnote to Table 2 for explanation of symbols.

with the predicted distributions for electric quadrupole absorption (Table 2) or from any of the channels listed in Table 3, unless one regards the experimental distribution to be either (i) wholly isotropic or (ii) made up of isotropic distributions contributed from various channels available in the tables plus a $\sin^2\theta$ component superimposed. Considering the higher energy group (Fig. 3 (*a*)), the distribution appears at variance with the predictions for the compound nucleus states listed in Tables 2 and 3. The distribution suggests a direct photoelectric interaction. The predicted angular distributions for the latter in the case of E1 absorption by a proton with initial angular momentum in the nucleus of l is:

$$\text{for transitions } l \text{ to } l+1: \quad \sigma(\theta)=2l+(l+2)\sin^2\theta, \quad \ldots\ldots \quad (5)$$

$$\text{for transitions } l \text{ to } l-1: \quad \sigma(\theta)=2(l+1)+(l-1)\sin^2\theta. \quad .. \quad (6)$$

Both types of transition are predicted by the theory of Courant (1951), while that of Wilkinson (1955) allows the "l to $l+1$" transition only. Thus the ejection of an "s" proton from the fluorine nucleus on these theories would lead to a $\sin^2\theta$ distribution in agreement with Figure 3 (*a*). It is significant that the ground state proton in ^{19}F has an *s*-wave designation on current nuclear shell theory.

Our results for the angular distributions can be compared with those of neighbouring light nuclei for the photon region below the giant resonance. On the one hand, the distributions for aluminium (Diven and Almy 1950) and magnesium (Toms and Stephens 1951) were found to be isotropic, or nearly so. On the other, the angular distribution for oxygen (Spicer 1955) was consistent with predictions involving compound nucleus formation, i.e. for the photon range 13·5–18·7 MeV, the distribution was consistent with E2 or M1 photon absorption. The difference in behaviour between oxygen and fluorine may well be due to the fact that the former is a closed shell nucleus while fluorine is a "closed-shell-plus-one" nucleus. The angular distribution of photoprotons from carbon at the giant resonance has been reported by Mann, Stephens, and Wilkinson (1955) who found their data was fitted best by predictions based on the independent particle character of the proton being ejected.

There is little to be gained from a detailed examination of the energy distribution of protons given in Figure 2. Owing to the density of levels and the inferior resolution, no conclusion can be drawn from it regarding the relative amounts of level absorption and continuous absorption of photons as required by the compound nucleus and independent particle interactions. The integrated cross section estimate of 18 MeV-mbarn for the photon range 10–16·5 MeV is comparable to that of the $^{19}F(\gamma, n)$ reaction in the same region, namely, 12 MeV-mbarn for the range 10·4–17 MeV (Horsley, Haslam, and Johns 1952).

V. Conclusions

The energy and angular distributions of the photoprotons from fluorine have been studied. The energy distribution does not provide evidence for absorption of photons by levels in ^{19}F. The angular distributions provide more

significant results. The higher proton energy group is best fitted with a $\sin^2\theta$ distribution which would be interpreted as a direct ejection of an "*s*" proton from the ^{19}F nucleus. This is consistent with the nuclear shell designation of the odd proton in fluorine. The angular distribution of the lower energy protons is more nearly isotropic and is not inconsistent with the predictions for the formation of intermediate compound nucleus states in ^{19}F. This distribution may be interpreted either as a mixture of direct photonuclear absorption and components from various channels listed in Tables 2 and 3, or, if solely due to compound nucleus formation in this region, as due to electric dipole or magnetic dipole absorption of photons by fluorine. The integrated cross section for the region studied is of the same order as that of the $^{19}F(\gamma, n)$ reaction for the same region.

VI. Acknowledgments

The authors wish to thank Professor L. H. Martin for his continued interest and advice during the course of the experiment. Thanks are also due to Dr. J. H. Smith of the University of Illinois and to Mr. B. M. Spicer for access to unpublished work and advice on the interpretation of the angular distributions.

VII. References

Ajzenberg, F., and Lauritsen, T. (1955).—*Rev. Mod. Phys.* **27**: 77.

Aron, W. A., Hoffman, B. G., and Williams, F. C. (1949).—Range-energy curves (2nd revision). U.S. Atomic Energy Commission Rep. A.E.C.U. 663.

Courant, E. D. (1951).—*Phys. Rev.* **82**: 703.

Diven, B. C., and Almy, G. M. (1950).—*Phys. Rev.* **80**: 407.

Drummond, J. E. (1955).—*Phys. Rev.* **97**: 1004.

Fuller, E. G. (1950).—*Phys. Rev.* **79**: 303.

Hirschfelder, J. O., and Magee, J. L. (1948).—*Phys. Rev.* **73**: 208.

Horsley, R. J., Haslam, R. N. H., and Johns, H. E. (1952).—*Phys. Rev.* **87**: 756.

Katz, L., and Cameron, A. G. W. (1951).—*Canad. J. Phys.* **29**: 518.

Katz, L., Haslam, R. N. H., Horsley, R. J., Cameron, A. G. W., and Montalbetti, R. (1954).—*Phys. Rev.* **95**: 464.

Levinger, J. S., and Bethe, H. (1950).—*Phys. Rev.* **78**: 115.

Lindhard, J., and Scharff, M. (1953).—*Math.-fys. Medd.* **27**, No. 15.

Livingston, M. S., and Bethe, H. (1937).—*Rev. Mod. Phys.* **9**: 263.

Mann, A. K., Stephens, W. E., and Wilkinson, D. H. (1955).—*Phys. Rev.* **97**: 1184.

Penfold, A. S., and Spicer, B. M. (1955).—*Phys. Rev.* (in press).

Spicer, B. M. (1953).—*Aust. J. Phys.* **6**: 391.

Spicer, B. M. (1955).—*Phys. Rev.* **99**: 33.

Titterton, E. W. (1955).—*Progr. Nucl. Phys.* **4**: 1.

Toms, M. E., and Stephens, W. E. (1951).—*Phys. Rev.* **82**: 709.

Wäffler, H. (1954).—"The Brown Boveri Betatron." p. 17. (Brown Boveri and Co.: Baden.)

Wilkins, J. J. (1951).—Range-energy relations for Ilford nuclear emulsions. A.E.R.E. Rep. G/R 664.

Wilkinson, D. H. (1955).—"Proceedings of the 1954 Glasgow Conference on Nuclear Physics." (Pergamon Press: London.)

Wilson, R. R. (1941).—*Phys. Rev.* **60**: 749.

APPENDIX I

Range-Energy Relation for Protons in Tetrafluoromethane (CF_4)

The range-energy relation in CF_4 has been calculated for proton energies from 0–10 MeV. For energies greater than 2 MeV, the usual Bethe-Möller formula for differential stopping power was used (Livingston and Bethe 1937). For low energy protons, an empirical treatment of the variation of stopping power adopted was similar to that of Lindhard and Scharff (1953).

Low Energy Region.—The stopping power B is given by the empirical relation

$$B/Z=a_1x^{\frac{1}{2}}+a_2x^{3/2}, \quad \ldots\ldots\ldots\ldots\ldots\ldots \text{(A1)}$$

where Z=atomic number of the material and $x=(v^2/2\alpha^2Z)$, v being the proton velocity and α the fine structure constant. The numerical values of a_1 and a_2 are fitted so as to give the experimental values of B/Z for air, and have the values $a_1=1\cdot40$ and $a_2=-0\cdot06$ for 2 MeV protons.

For a molecule with s_i atoms of atomic number Z_i, and stopping power B_i, the effective stopping power

$$B_e=\sum_i s_iB_i. \quad \ldots\ldots\ldots\ldots\ldots\ldots \text{(A2)}$$

Now the energy loss of protons in a gas under standard conditions is given by (Hirschfelder and Magee 1948)

$$\mathrm{d}E/\mathrm{d}R=-0\cdot006094(B/E). \quad \ldots\ldots\ldots\ldots \text{(A3)}$$

These expressions can be combined to give for the differential stopping power in MeV/cm:

$$\mathrm{d}E/\mathrm{d}R=-0\cdot006094\eta a_1E^{-\frac{1}{2}}(1+kE)\sum_i(s_iZ_i^{\frac{1}{2}}), \quad \ldots\ldots \text{(A4)}$$

where

$$\eta=\alpha^{-1}(2/Mc^2)^{\frac{1}{2}}=6\cdot327,$$

and

$$k=\eta^2(a_2/a_1)(\sum_i s_iZ_i^{-\frac{1}{2}})/(\sum_i s_iZ_i^{\frac{1}{2}}),$$

$$\alpha=1/137,$$

$$Mc^2=938\cdot2 \text{ MeV}.$$

In the case of CF_4, $k=-0\cdot0551$.

Integrating equation (4) leads to an expression for the range

$$R=\frac{2}{3}\,\frac{E^{3/2}}{0\cdot5571a_1}\left(1-\frac{3}{5}kE+\frac{3}{7}k^2E^2\right), \quad \ldots\ldots\ldots \text{(A5)}$$

which gives the value $R=2\cdot59$ cm for $E=2$ MeV.

High Energy Region.—The differential stopping power in this region was calculated in the usual way from the Bethe-Möller formula

$$\frac{\mathrm{d}E}{\mathrm{d}R}=-\frac{4\pi e^4z^2}{mv^2}NZ\left\{\ln\frac{2mv^2}{I}-\ln(1-\beta^2)-\beta^2\right\}, \quad \ldots\ldots \text{(A6)}$$

using a value of $k' = I/Z = 11 \cdot 5$, as found for air and aluminium by Wilson (1941). The differential stopping powers for carbon were taken from the tables of Aron, Hoffman, and Williams (1949), and the values for fluorine were calculated in a similar way. By means of the usual assumption that the differential stopping powers are additive, the range-energy relation for CF_4 was obtained by numerical integration for protons with energy between 2 and 10 MeV.

Combining this with the lower energy determination, the values of differential stopping power and range are listed in Table 4.

TABLE 4

DIFFERENTIAL STOPPING POWER AND RANGE-ENERGY RELATION FOR CF_4 AT 15 °C AND 760 MM HG

Proton Energy (MeV)	Stopping Power relative to Air	Range (cm)
0	2·69	0
0·5	2·70	0·30
1	2·71	0·85
2	2·73	2·59
3	2·76	5·01
4	2·78	8·14
5	2·79	11·93
6	2·81	16·37
7	2·81	21·43
8	2·82	27·10
9	2·82	33·36
10	2·83	40·21